Finally, we calculated the output waveforms from SRR-SSM and CRR-MZM for a 50-Gb/s pseudorandom binary sequence (PRBS) of 2^7-1. In the calculation, we used the same procedure as that described in section 3.1. The use of Eqs. (16) to (18) is not limited within small signal analysis and is valid for large signal modulation. Therefore, we simply applied the input signals of PRBS to those equations and the procedure to calculate eye diagrams. We set the rise and fall time to be 5.9 ps for the transition between 0 and 1 state with the thresholds of 10 and 90%, respectively. This rise/fall time was large enough for the round-trip time of 0.67 ps. By using Fig. 7(a), we determined the photon lifetimes of the RRs used in the two device configurations, respectively, such that both devices had the same 3-dB bandwidth of about 40 GHz. With this constant 3-dB bandwidth, it is expected that both devices equally show sufficient qualities of eye diagrams for 50-Gb/s operations. Thus, it is possible to evaluate the modulation depths of the two devices and compare them for 50-Gb/s operations. Choice of the smaller 3-dB bandwidth and the longer photon lifetimes would cause inadequate qualities of eye diagrams for 50-Gb/s operations. Figures 8(a) and (b) show the resulting eye diagrams, with the parameters used in the calculation shown in the graphs. By cascading 4-RRs with a relatively small photon lifetime, the CRR-MZM provided an eye opening that was wider than that of the SRR-SSM.

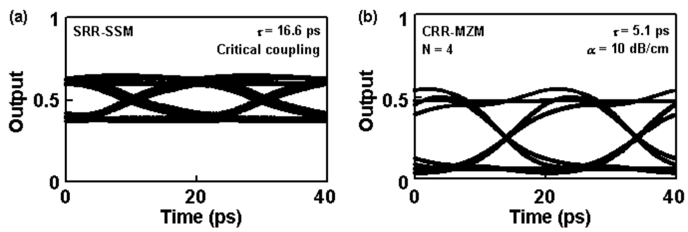

Fig. 8. Calculated outputs as eye diagrams for 50-Gb/s PRBS signal of 2^7-1. (a) SRR-SSM (b) CRR-MZM with $N = 4$ (b).

4. Conclusion

We investigated the high-speed modulation characteristics of CRR-MZMs using analytical and numerical calculations. We derived an analytical formula for the small-signal response of CRR-MZM based on TCM theory, for which we numerically confirmed the validity. The analysis indicated that CRR-MZMs had a maximum operating bandwidth when proper delays were set in the applied electrical signals between neighboring RRs. The optimized delay was equal to twice the photon lifetime of each RR.

We determined the performances of both CRR-MZMs and standard SRR-SSM for a wide variety of parameters, including the photon lifetime of RRs, the number of RRs cascaded, and the propagation loss of the RR. We compared the results between those two device configurations in terms of the modulation depth and bandwidth. For a given magnitude of the waveguide index change, CRR-MZM can provide a larger modulation response than an SRR-type modulator in a frequency range greater than 25 GHz. The results showed the advantage of CRR-MZM over SRR-SSM in designs aimed at providing a larger modulation response at high-operating frequencies.

Acknowledgments

The authors would like to thank Tatsuya Usuki for the helpful discussions and suggestions that he made. The authors also acknowledge valuable assistance from Tsuyoshi Yamamoto.